HH 110 Jet Near Infrared I aging. The Outflow Mixing Layer?

A Noriega-Crespo

Infrared Processing and Analysis Center, CalTech-JP , Pasadena, CA 91125

P. Garnavich

Harvard-Smithsonian Center for Astrophysics, Cambridge, MA 02 38

A.C. Raga & J Cantó

Instituto de Astronomia, UNA Mexico D 04510

and

K.-I öhm

Department of Astronomy, University Washington, Seattle, WA 98 95

To be submitted
to the Astrophysical Journal

HH 110 Jet Near Infrared Imaging. 1. The Outflow Mixing Layer?.

A. Noriega-Crespo
Infrared Processing and Analysis Center, CalTech-JPL, Pasadena, CA 91125
email: alberto@ipac.caltech.edu

P. M. Garnavich
Harvard-Smithsonian Center for Astrophysics, Cambridge, MA 02138
email: peterg@cfanewton.harvard.edu

A.C. Raga
Instituto de Astronomia, UNAM, Mexico DF 04510
email: raga@astroscu.unam.mx

J. Cantó
Instituto de Astronomia, UNAM, Mexico DF 0151()
email:canto@astroscu.unam.mx
and

K.-H. Böhm
Department of Astronomy, University of Washington, Seattle, WA 98195
email: bohm@astro.washington.edu

1{ eceived _____ .——..—.; accepted——...—-..— ————

A 3S' 'RACT

We present near infrared images of the Herbig-Haro 110 jet centered at the molecular hydrogen ines $v = 1 - 0$ 2.121 μm and $v = 2 - 1$ 2.248 μm. In YSOs these lines are mostly excited by low velocity shocks and the energy released by turbulent processes. The ratio of these of lines provides us with a preliminary diagnostic of the molecular gas excitation. The H 110 jet was selected for four reasons: (i) it has a complicated optical 'turbulent' morphology, (ii) it is close to a high density circumstellar environment (a molecular core), (iii) this object does not have an obvious driving source, and (iv) theoretical models suggest that this object corresponds to the early stages of a jet-cloud collision

We find that the molecular ydrogen emission follows the optical α and [SII] emission for a 'straight' section of the jet of $\sim 1'$, but it becomes shifted westward and separated from the optical emission afterwards. The 2.248 μm emission is fain n most condensations, except for the knots B1, E1 and P1 where it is clearly detected We suggest that the morphological properties of the nolecular hydrogen emission are consistent with t rat of a boundary layer. The ratio of the (1,0) S(1) 2.121 to (2,) S(1) 2.248 lines ranges from 0.9 to 7.5 along the jet, indicating a non-isothermal structure. In those cases where the H_2 emission is ikely to be due to shocks the line ratios are small enough to be explained either by C or J-type shocks.

1. Introduction

Near infrared narrow band imaging of Herbig-Haro objects and jets has proven to be a powerful tool to determine the morphology of the interaction region between the stellar jet (of mostly atomic gas) and its molecular environment. It has been suggested (Raga et al. 1993, Raga & Cabrit 1993) that in some cases this interaction can be strongly coupled and that the fast highly collimated stellar jet may be able to drive the slower and more poorly collimated molecular outflow (e.g. HH 46/47, Eislöffel et al. 1994). The coupling between the outflows is done through low velocity shocks and by turbulence/mixing/entrainment (see e.g. Raga 1995).

In HH objects the energy released during the jet/environment interaction can excite molecular hydrogen. The H_2 $v = 1 - 0$ S(1) line at 2.121 μm, for instance, is relatively bright and has been used to map several of the outflows. Among some **of** the most recent examples of the application of this technique we find HH 1 - 2 (Davis, Eislöffel & Ray 1994, Noriega-Crespo & Garnavich 1994), 11117-11 (Stapelfeldt et al. **19!)]),** HH 46/47 (Eislöffel et al. 1994), 1111 43/54/56/99A/1 06/12[) (Gredel 1994), 1111 111/121(Gredel & Reipurth 1993) and 1111 110/111/91(Davis, Mundt & Eislöffel 1994). In some cases, the jets are **not** detected at optical wavelengths, but they are clearly seen in the H_2 lines, for instance, L1448 (Bally, Lada & Lane 1993, Davis & Smith 1995) and HH 211 (McCaughrean, Rayner & Zinnecker 1994).

In conjunction with the H_2 2.121 μm line, it possible to use the H_2 $v = 2 - 1$ S(1) 2.248 μm line to determine the excitation of the molecular gas and the likely mechanisms that lead to it (e.g. see Wolfire & Königl 1991 for details). The 2.248 μm line can be a factor $\sim 3 - 20$ times fainter than the 2.12 μm line (depending on the excitation process), and for this reason has been less often observed and studied using narrow band imaging.

In this study we present NIR narrow band images of HH 110 taken in the 2.121 μm and 2.248 μm molecular hydrogen lines, in order to determine its excitation, its relationship to

the optical emission, and the likelihood that this emission originates in a mixing layer. The HH 110 jet was selected because of its complicated optical 'turbulent' morphology (Reipurth & Olberg 1991, Reipurth, Heathcote & Raga 1995), which is very different from that observed at 2.12 μm (Davis, Mundt & Eislöffel 1994). At 2.12 μm the jet is nearly straight and shifted westward from the optical emission (Raga 1995), suggesting that the molecular H_2 emission arises from a jet-cloud collision, perhaps at its boundary layer (Raga & Cantó 1995a). Also, the proper motion and radial velocity measurements of Reipurth et al. (1995) are consistent with such a jet-cloud collision scenario for HH 110.

2. Observations and Data Reduction

The observations were carried out with the 3.5m telescope at Apache Point Observatory, on February 18 & 26, 1995. We use as detector a 256×256 RISC CCD with a scale of $0.''482$ pixel^{-1} at f/5, which gives a field of view of $\sim 2' \times 2'$. The filters used were centered at 2.121 μm (H_2 $v = 1 - 0$), 2.248 μm (H_2 $v = 2 - 1$), and 2.22 μm (continuum), with FWHM transmissions of 1%, 2% and 4% respectively.

The images were created by a mosaic of 9 (2.12 μm) and 13 (2.25 μm) spatially contiguous frames, with integration times of 180 sec per frame, and a FWHM resolution between $1'' - 1.''5$. The data were reduced in the following way. A mean dark frame with an exposure time of 240 seconds was subtracted from each science exposure and the result divided by a normalized flat field constructed in both filters from images of the illuminated dome. A sky frame was created by removing the bright emission objects from each data frame (substituting the average local sky) and taking a median of the images after adjusting for slight differences in the overall sky level. The sky frame was then scaled and subtracted from each data image so that the background was near zero. Because of independent variations in the four amplifiers on the chip, residual levels in each quadrant had to be removed individually to bring the entire frame background to a mode of zero.

Pixel shifts to bring all the frames to the same center were measured by centroiding on the bright stars. The bad pixels in the images were then masked, the images expanded by a factor of six and shifted to the nearest integer pixel. The results were resampled to their original size while ignoring the previously masked pixels. Software for these operations was provided by M. Rieke and C. Engelbracht (private communication). Nine data frames in the 2.12μm filter and 13 images in the 2.25μm filter were averaged using a 3-sigma rejection algorithm to produce the final results.

Scheduling constraints at APO prevented us from observing standard stars on February 18, when the HH110 data were obtained. The IR standard HD18881 (Elias et al. 1982) was observed the following night under rather poor conditions, and we estimate that our flux calibration is accurate to within only a factor of two (see Table 1).

The morphology of the H_2 emission is compared (following section) with that of the optical emission in Hα and [S II] 671 7/31. These images were kindly provided to us by Bo Reipurth, were taken with the 3.5m NTT in January, and have a sub-arcsecond resolution. For details we refer the reader to Reipurth et al. (1995).

The Hα and [S II] images were transformed to the H_2 image coordinates using the geomap/geotrans routines in IRAF.[1] . Six stars in common to all the frames were used to determine the linear (rotation, magnification and translation) transformation coefficients and the RMS solution residuals were of less than 0.1 pixel.

3. Results and Discussion

The HH 110 jet was first studied by Reipurth & Olberg (1 991) at optical wavelengths, and the nomenclature for the knots is taken from this pape Very recently Davis et al. (1 994)

[1] Image Reduction and Analysis Facility is distributed by the National Optical Astronomical Observatory

provided us with the first N R images at 2.12 μm and K band, and new sub-arcsecond images in Hα and [S II] 6717/31 Å have been recently obtained by Reipurth et al. 1995), who studied the structure and proper motions of HH 0, and its relationship to HH 270. One of the most striking features of 0 is the differen orphology of its optical and NIR emission and their clear demarcation, with the H_2 shifted wes ward fro n the optical emission in the most turbulent region (see Fig. 1). The searc for the 0 d ving source in FI R and submillimiter wavelengths along its outflow axis has so far been unsuccessfu (Reipurth et al. 1995). The morphological differences and absence of a source have led to the suggestion that in 0 we are witnessing a "grazing" jet-cloud core collision (Reipurth et al 1995, Raga 995, Raga & Cantó 1995b, and see below).

f the morphology of HH 110 is indeed the result of a grazing collision, then the displacement of the molecular emission with respect to the optical emission could be explained in terms of a boundary or mixing layer. In this scenario, as some of the jet flow "bounces" back and forth away from the cloud core, simultaneously some of the gas 'slides' underneath and closer o r c core creating a zone where atomic and molecular gas interact (Raga & Cantó 995a) The H_2 emission could be tracing his region (see Fig.). If is is the case, owever, models of the energy release through turbulent eddies, the excitation of the molecular gas and the prediction of the emitted H_2 spectrum do not exit at the moment. The available simplified nodels of the chemical atomic and molecular properties of a turbulent layer, nevertheless, predict hat a large fraction of the energy goes into the excitation and emission of H_2 (Taylor & Raga 1995). Some of the brightest H_2 knots, e.g. B1, E1 and P1, however, follow quite closely the optical emission and resemble bow shock structures. Also, we should note the complete absence of knot C in H_2 in ig. 2. For these condensations probably most of the radiation arises from shock excitation, and some insight may be obtained by making a comparison with available shock models (see below)

3.1. Fluxes and Line Ratios

The measured surface brightness (σ) within a $\sim 6''$ aperture ($\sim 5^2$ pixel^2), as well as the ratio of the 2.121 μm to 2.248 μm lines are presented for each knot of the 110 jet in Table 1. As mentioned before, we estimate that the fluxes in both lines are correct to within a factor 2. The uncertainties in the ratios were determined by estimating the nearby sky and noise corresponding to each knot, also within a $\sim 6''$ aperture. The 2.12/2.25 ratio varies from 0.9 (knot N1) to 7.6 (knot B1), with 8 of 13 knots with values between 3.0 to 8.0. The most reliable ratios are those for the brightest knots, i.e. B1 (7.6), E1 (4.5), H1 (1.9), I2 (2.6) and P1 (7.0).

It is possible, as a first approximation, to assume that the (1,0) S(1) and (2,1) S(1) levels have been populated in near local thermodynamic equilibrium, and therefore can be described according to a Boltzmann factor (Scoville et al. 1982, Gredel, Reipurth & Heathcote 1992, Smith 1994a), which it is probably correct when the gas density is relatively high, $> 10^5$ cm^{-3}. In this situation the H_2 "excitation" temperature is inversely proportional to the 2.12/2.25 ratio. The ratios in the range 4.5 - 7.6 correspond to temperatures $\sim$ 2400 - 3100 K, while the smaller ratios 0.9 - 1.6 correspond to temperatures $\sim$ 4460 – 5950 K. Under these conditions the jet is not isothermal, although three of the brightest knots, i.e. B1, E1 and P1, have very similar temperature values.

A detailed comparison with more sophisticated shock models truly requires spectroscopic information. In the case of L1448, one of the few outflows in which both 2.121 μm and 2.248 μm have been observed (Davis & Smith 1995), for instance, it has been shown that the standard molecular shock models, either J or C type, have problems in predicting large values for the 2.12/2.25 ratio (i.e. $\gtrsim 10$), but smaller values can be obtained in several ways in the *high density regime*. There is a tendency to prefer J-type molecular shock models rather than C-type, because the latter ones depend on several parameters such as gas density, oxygen abundance and ionization fraction (Smith 1994a,b).

We can estimate readily the energy released in the H_2 2.121 μm line, infer from this the total luminosity per unit length, and to compare with the predictions of the available models (Cantó & Raga 1991). The surface brightness over the straight arc minute of the jet in the (1,0) 2.121 μm line is $\sim 3.3 \times 10^{-15}$ erg s^{-1} cm^{-2} arcsec^{-2}, that over an area of ~ 125 arcsec^2 corresponds to a flux of $\sim 4 \times 10^{-13}$ erg s^{-1} cm^{-2}, which at a distance of 460 pc to Orion gives an energy radiated $L_{2.12} \sim 10^{31}$ erg s^{-1}. Assuming that the 2.12 μm line carries $\sim 1/6$ of the total H_2 energy radiated (Brand et al. 1988), then $L_{H_2} \sim 0.016\ L_\odot$. This energy per unit length in the straight arc minute of the HH 110 jet is therefore $\sim 0.11\ L_\odot$. The radiated energy per unit length per unit time in a two-dimensional mixing layer is given by (Cantó & Raga 1991)

$$l = 0.028 \left(\frac{L_\odot}{\mathrm{pc}}\right) \left(\frac{T_j}{10^4 \mathrm{K}}\right)^{1/2} \left(\frac{n_j}{10^3 \mathrm{cm}^{-3}}\right) \left(\frac{v_j}{100 \mathrm{kms}^{-1}}\right)^2 \left(\frac{r_j}{10^{16} \mathrm{cm}}\right), \quad (1)$$

where T_j, n_j, v_j and r_j are the jet temperature, density (atoms and ions), velocity and radius, respectively. The overall HH 110 flow velocity is ~ 83 km s^{-1} (Reipurth et al. 1995), so for standard values $T_j = 10^4$ K and $r_j = 10^{16}$ cm, a density of $\sim 5 \times 10^3$ cm^{-3} provides a value consistent with the observations ($\sim 0.1\ L_\odot$ pc^{-1})

3.2, Spatial Intensity **Distribution**

The H_2 and optical morphologies are very similar in the initial arc minute of the jet. If the H_2 emission arises from a mixing layer, however, we expect some subtle differences along its cross section to take place (Cantó & Raga 1991, Raga, Cabrit & Cantó 1995). Furthermore, differences between the H2 and Hα -[S II] emission are also expected in those knots with a bow shock-like morphology (Raga et al. 1995), due to dissociation of H_2 at speeds ≥ 50 km s^{-1}which can be reached at the bow shock apex. In figures 3 and 4 we show the intensity distributions of the optical (Hα and [S II]) and H_2 emission in this region along

and perpendicular to the flow axis, in order to study this possibility.

The intensity along the jet flow axis is shown in Figure 3. The curves represent the integrated emission within a 4.″3 aperture across the jet and along its flow axis between the knots A and H. Because of the aperture size the bright optical knot E is not included.

From Figure 3 it is evident that there is resemblance between the molecular and the optical emission, but they are by far not identical even in this section of the jet. We immediately note that among the strongest optical knots, B and H have H_2 counterparts, but knots A and C do not have. These two later ones resemble slightly "bent" bow shock structures (see Fig. 2), and perhaps the H_2 emission is created behind them, i.e. in knots A1 and C1. This is particularly interesting for knot A, since the H_2 jet extends northwards about $\sim 5''$ more than the optical one (Fig. 3). Knot A could be tracing the initial interaction between the jet and the molecular core.

Figure 4 shows the intensity distribution perpendicular to the flow axis and along the cross section of the jet, which it is quite relevant for a boundary layer. Among the predictions of the mixing layer structure in a stellar jet (Cantó & Raga 1991), there is that of the fraction of molecular and atomic hydrogen as a function of position along the cross section (see sec. 3.3) Under the assumption that the viscous turbulence is independent of the position across the mixing layer, then the fraction of hydrogen in H_2 should reach a maximum value near the molecular cloud (~ 1) and it should decrease linearly to a minimum value closer to the atomic jet (~ 0). Furthermore, the emission from this layer should reflect directly this hydrogen fraction, since its structure across is essentially isothermal and in transverse pressure equilibrium (see Appendix A). The intensity distribution along the jet cross section shows precisely this tendency (see Fig. 4). The H_2 emission is confined within FWHM$\sim 3''$, while the atomic Hα and [S II] emission have extended "wings" eastwards for approximately another $5''$.

Davis et al. (1994) have interpreted their H_2 observations as showing the presence of a laminar molecular jet in the less turbulent region of the mixing layer, i.e. closer or inside

the atomic jet, while the optical emission arises from the most turbulent regions where the shear is the greatest. It is clear that the observed offset between the optical and molecular emission does not grant this interpretation. The molecular H_2 jet is indeed 'straight', but it is definitively closer to the molecular cloud.

3.3. **Theoretical** interpretation

Reipurth et al. (1995) have presented a detail analysis of the proper motions and radial velocities of HH 110, and concluded that this object very probably corresponds to the same flow as the HH 270 jet (which has a roughly E-W direction), which is being deflected to a roughly N-S direction through a collision with a dense obstacle. Theoretical models for this deflection process have been developed by Raga and Cantó (1995a).

Even though these models can correctly explain the difference in the kinematical properties of HH 270 and HH 110 (Heathcote et al. 1995), they fail to explain the sudden brightening that occurs at the collision point, where the faint HH 270 jet is deflected to become the much brighter HH 110 outflow. This conspicuous lack of success of the jet deflection model suggests that the emission of HH 110 might arise in a turbulent mixing layer generated in the jet/cloud collision region, an effect which is not considered in the theoretical models. Raga and Cantó (1995b) point out that the E-W spatial offset between the Hα and H_2 1 – 0 S(1) lines might be consistent with what one would expect from a mixing layer between an atomic jet and a molecular environment. This mixing layer would be present only on the *W* side of the HH 110 jet, since this is the side that is in contact with the dense, molecular obstacle close to the deflection point (*i. e.*, the beginning of the HH 110 jet).

If one carries out a simple, analytic model for the spatial structure of a mixing layer (see Appendix A), one finds that the temperature cross section of the mixing layer has a large isothermal plateau (see figure 5). Also, one finds that the Hα emission peaks close to the edge of the jet beam, and that the H_2 1 – 0 S(1) peaks close to the interface between the mixing

layer and the undisturbed, molecular environment (see figure 6, and Appendix A).

This simple model shows that the offset between the molecular and atomic emission observed in HH 110 is indeed consistent with a scenario in which the H_2 emission arises in a turbulent mixing layer between an atomic jet (on the E side of HH 110), and a molecular environment (on the W side of HH 110). Of course, our simple, analytic model (see Appendix A) makes no prediction whatsoever of the details of the clumpy spatial structure that is observed in the emission of HH 110.

Acknowledgements

A.N.-C. research is supported by NASA Long Term Astrophysics program through a contract with the Jet Propulsion Laboratory (JPL) of the California Institute of Technology. It is a pleasure to thank Bo Reipurth & Steve Heathcote for kindly making available to us their NTT HH 110 images prior to publication. We thank the staff of the Apache Point Observatory for their support during the observations.

Appendix A

Cantó and Raga (1991) developed a simple model describing the properties of the flow averaged across the width of a turbulent mixing layer. Taylor and Raga (1995) extended this model by including a detailed chemical network that was solved self-consistently w th the flow equations. These .wo papers show that except in the region very close to the source (where the mixing layer is very narrow), the resulting flow is basically isothermal, with a temperature of $T_0 \sim 12000$ K. This result directly reflects the fact that the cooling curve has a very steep rise at these temperatures, due to collisional excitations of the Lyman-α line.

Let us now write the equation that describes the thermal structure of the cross section of a turbulent mixing layer. f one neglects the terms nvolvi ıg gradients along the direction of the flow, this equation takes t ıe simple form

$$\mu \left[\frac{C_p}{P_r} \frac{d^2T}{dy^2} + \left(\frac{dv}{dy} \right) \right] = - L , \qquad (\hat{} \ )$$

where μ is the turbulent viscosity, C_p is the specific heat (per unit mass at constant pressure, L is the radiative energy loss per unit volume, and $v(y)$ is the velocity along the direction of the flow as a function of the coordinate y, which is measured outward from the jet into the mixing layer. $P_r = \mu C_p / \kappa_c$ (where κ_c is the turbulent conductivity) is the turbulent Prandtl number, which is found to have values close to unity in laboratory experiments (see, e. g., Bradshaw 1977). For derivi ıg equation (1) it has also been assumed that both κ_c and C_p are independent on the position y across the mixing layer

Following Cantó and Raga (1991), we now consider that the velocity cross section of a turbulent mixing ayer is closely follows the cross section of a plane, Couette flow

$$v(y) = v_j \left(- \frac{y}{h} \right) , \qquad \text{A2}$$

where v_j is the velocity of the jet and h is the tota width of the mixing layer.

Using equation (2) and setting $P_r = 1$, equation 1) can be rewritten as :

$$\frac{1}{\gamma - 1}\frac{d^2t}{d\eta^2} + 1 = -\frac{Lh^2}{\mu v_j{}^2}, \tag{A3}$$

where we have defined a dimensionless temperature $t = T/T_0$ (where $T_0 \approx 12000$ K is the temperature around which the radiative cooling grows very rapidly, see above) and a dimensionless coordinate $\eta = yM_j/h$ measuring the position across the mixing layer ($\eta = 0$ corresponding to the jet/mixing layer boundary, and $\eta = M_j$ corresponding to the mixing layer/undisturbed environment boundary). The Mach number is defined as $M_j = v_j/c_0$, where c_0 is the adiabatic sound speed at the temperature T_0.

It is possible to obtain a simple, analytic integral of equation (A3) if one idealizes the radiative cooling term as :

$$L = 0\,;\ \ T \leq T_0\,, \tag{A4a}$$

$$L = \infty\,;\ \ T > T_0\,, \tag{A4b}$$

which is a straightforward simplification of the steep rise of the cooling function around $T \approx T_0$.

With this simplified cooling function, equation (A3) can be integrated in a straightforward way. The solution has two different regimes :

regime a : for $M_j \leq \sqrt{3(1 - t_j)} + \sqrt{3(1 - t_e)}$ (where t_j and t_e are the dimensionless temperatures of the jet and the environment, respectively) the mixing layer does not attain a temperature high enough for the radiative energy loss to play a role, so that an adiabatic solution is obtained :

$$t(\eta) = t_j + \left(\frac{t_c - t_j}{M_j} + \frac{M_j}{3} \right) \eta - \frac{1}{3}\eta^2 . \qquad (A5)$$

regime b : for $M_j > \sqrt{3(1 - t_j)} + \sqrt{3(1 - t_c)}$ the central region of the mixing layer does reach a temperature T_0, and an isothermal plateau of dimensionless temperature $t = 1$ is formed. The solution of in this case takes the form :

$$t(\eta) = t_j + \frac{2}{3}\eta_j \eta - \frac{1}{3}\eta^2 ; \quad 0 \leq \eta < \eta_j , \qquad (A6a)$$

$$t(\eta) = 1 ; \quad \eta_j \leq \eta \leq \eta_c , \qquad (A6b)$$

$$t(\eta) = t_c + \frac{2}{3}(M_j - \eta_c)(M_j - \eta) - \frac{1}{3}(M_j - \eta)^2 ; \quad \eta_c < \eta \leq M_j , \qquad (A6c)$$

where $\eta_j = \sqrt{3(1 - t_j)}$ and $\eta_c = \sqrt{3(1 - t_c)}$ are the positions of the two edges of the isothermal plateau of the mixing layer cross section (see figure 5). For deriving equations (A5) and (A6), we have assumed a constant value $\gamma = 5/3$ for the specific heat ratio (which is clearly only a rough approximation for the case of a mixing layer between an atomic jet and a molecular environment).

For an HH jet, we have relatively high Mach numbers $M_j \sim 10$, so that the mixing layer is clearly in the radiative *regime b* . This leads to a temperature cross section of the mixing layer such as the one shown in figure 5, which has been computed for a model with $M_j = 10$, $t_j = T_j/T_0 = 0.3$, and $t_c = T_c/T_0 = 0.1$. These values have been chosen in order to show the characteristics of our analytic solutions.

It is also possible to use simple arguments to determine the dependence of the Hα and H_2 1 – 0 S(1) emission across the width of the mixing layer. The turbulent diffusion will lead to approximately linear dependences of the fraction of hydrogen nuclei in atomic or ionic (H)

and molecular (H_2) form as a function of the dimensionless position η, with an abundance of 1 for H (and 0 for H_2) at $\eta = 0$ (*i. e.*, at the laminar jet/mixing layer boundary) and 0 for H (0.5 for H_2) at $\eta = M_j$ (*i. e.*, at the mixing layer/undisturbed environment boundary).

These linear dependences of the fractions of H and H_2 as a function of position across the mixing layer will of course be modified by the presence of destruction (*i. e.*, collisional ionization and dissociation) processes in the mixing layer. However, the detailed calculations of Taylor and Raga (1995) show that these processes do not play an important role in mixing layer flows.

In order to calculate an approximate form for the dependence of the Hα emission across the mixing layer we furthermore assume that the Hα emission is dominated by collisional excitation from the ground state. With this assumption, and considering the temperature dependence of the collisional excitation coefficient, we finally obtain a dimensionless Hα emission of the form :

$$I_{H\alpha}(?/) = \left(1 - \frac{\eta}{M_j}\right)^2 \left(2 - \frac{\eta}{M_j}\right)^{-2} t^{-5/2}\, e^{11.7(1-1/t)}, \qquad \text{(A7)}$$

where the dimensionless temperature t is given as a function of η by equations (5-6), and we have assumed that the cross section of the mixing layer is in lateral pressure equilibrium.

To calculate the dependence of the H_2 1 – 0 S(1) emission on position across the mixing layer, we assume that collisions with H atoms or ions, or with other H_2 molecules have identical contributions to the population of the upper level of this transition. We then obtain :

$$1\,1\,1_2 1\text{-}\,0S(1)(\eta) \left(\frac{\eta}{M_j}\right)\left(2 - \frac{\eta}{M_j}\right) t^{-5/2}\, e^{0.57(1-1/t)} \qquad \text{(A8)}$$

The results from equations (A7) and (A8) are shown in figure 6, for a model with $M_j = 10$, $t_j = 0.3$ and $t_e = 0.1$. These emission cross sections are compared with observations of the HH 110 outflow in section 3.3 of this paper.

REFERENCES

Bally, J., Lada, E. A., & Lane, A.P. 1993, ApJ, 418, 322

Bradshaw, P. 1977, *Ann. Rev. Fluid* Aft'c}/., 9, 33.

Brand, P. W. J.L., Moorhouse, A., 11111'1011, M.G., Geballe, T.R., Bird, M., & Wade, R. 1988, ApJ, 334, **1,103**

Cantó, J., & Raga, A . C. 1991, ApJ , 372, 646

Davis, C. J., Eislöffel, J., & Ray, '1'.1'. 1994, ApJ, 426, L93

Davis, C .J., Mundt, R., & Eislöffel, J. 1994, ApJ, 437, L55

Davis, C.J., & Smith. M.D. 1995, ApJ, 443, 1,41

Eislöffel, J., Davis, C .J., Ray, T.P., & Mundt, R. 1994, ApJ, 422, L91

Elias, ,1.11., Frogel, J. A., Matthews, K., & Neugebauer, (i, 1982, AJ, 87, 1029

Gredel, R., Reipurth, B., & Heathcote, S. 1992, A&A, 266, 439

Gredel, R., & Reipurth, B. 1993, ApJ, 407, L29

Gredel, R. 1994, A&A , 292, 580

Heathcote, S., Reipurth, B., & Raga, A .C. 1995 (in preparation)

McCaughrean, M .,1., Rayner, ,1.'1'., & Zinnecker, H. 1994, ApJ, 436, L189

Noriega-Crespo, A. & Garnavich, P.M. 1994, AJ, 108, 1432

Raga, A.C. 1995, RMxAASC, 1, 103

Raga, A. C., and Cantó, J. 1 995a, RM xAA, 35, 51

Raga, A.C ., and Cantó, J, 1995b, R MxAASC (in press)

Raga, A .C., Cabrit, S., & Cantó, J. 1995, MNRAS, 273, 422

Raga, A. C., & Cabrit, S. 1993, A&A, 278, 267

Raga, A. C., Cantó, ,J., Calvet, N., Rodríguez, L.F., Torrelles, J.M. 1993, A&A, 276, 539

Raga, A. C., Taylor, S.D., Cabrit, S., & Biro, S. 1995, MNRAS (in press)

Reipurth, B., & Olberg, M. 1991, A&A, 246, 535

Reipurth, B., Heathcote, S., & Raga, A.C. 1995, A& A (subm tted)

Scoville, N, Z., Hall, D.N.B., Kleinmann, S. C., & Ridgway, S.' '. 1982, ApJ, 253, 136

Smith, M1). 1994a, A&A, 289, 256

Smith, M.D. 1994b, MN R AS, 266, 238

Taylor, S.D., & Raga, A.C. 1995, MNRAS (in press)

Stapelfeldt, K.R., Beichman, C.A., Hester, J.J., Scoville, N.Z., & Gautier, T.N. 1991, ApJ, 371, 226

Wolfire, M.G., & Königl, A. 1991, ApJ, 383, 205

This manuscript was prepared with the AAS LaTeX macros v3.0.

Table 1, 1111 110112 Line Ratio

Knot	$\sigma(2.12)^{a,b}$	$\sigma(2.12)/\sigma(2.25)^{b}$
A1	0.5	5.7 ± 3.4
A2	0.6	r).] ± 3.0
B1	1.1	7.6 ± 4.0
C1	0.3	2.8 ± 2.2
E1	1.4	4.5 ± 1.0
111	0.8	1.93- 0.2
11	0.2	4.8 ±1.6
I2	0.4	2.6 ± 1.7
13	0.3	1.5 ± 1.0
M1	0.2	3.7 ± 3.5
N1	0.1	0.9 ± 1.0
P1	1,0	7.0 ± 3.6
Q1	0.3	3.3 ± 2.7

“ in 10^{-18} W m^{-2} ar csec^{-2}

[b] with in $\sim 6''$ aperture

Figure Captions

Figure 1 - *(a)* A grayscale image of the HH 110 jet in the H_2 2.121 μm emission line. The field is $\sim 2'$, north us up and east is left. *(b)* A superposition of the H_2 2.121 grayscale image and the optical emission in Hα (contours). Both molecular and atomic components seem to arise in a common region in the straight part of the jet (north), but they become clearly separated further south, where the optical jet becomes quite 'turbulent'.

Figure 2 - A grey scale image of the straight section ($\sim 1'$ long) of the HH 110 jet in the 2.121 μm, 2.248 μm and Hα emission lines.

Figure 3 - The spatial intensity distribution along the HH 110 jet flow axis in its straight region across a 4."3 aperture of the H_2 emission (top) and the Hα and [S II] emission (bottom).

Figure 4- The spatial intensity distribution of H_2, Hα and **[S II]** 6717/31 perpendicular to the flow axis and along the cross section of knots in the straight section of the HH 110 jet, within a $\sim$ 1 5" aperture.

Figure 5 - Dimensionless temperature $t = T/T_0$ (where $T_0 = 12000$ K is the temperature at which the radiative cooling has a steep rise) as a function of the dimensionless position $\eta = y\,M_j/h$ across the mixing layer (see the text). At $\eta = 0$, t is equal to the dimensionless temperature $t_j = T_j/T_0$ of the jet, and at $\eta = M_j$, t is equal to the dimensionless temperature $t_e = T_e/T_0$ of the undisturbed environment. For $\eta_j < \eta < \eta_e$, the mixing layer has an isothermal region with $t = 1$. The solution shown in this figure was calculated for a model with $M_j = 10$, $t_j = 0.3$ and $t_e = 0.1$.

Figure 6 - Dimensionless Hα (solid line) and $H_2$1 - 0 S(1) emission (dotted line) as a function of dimensionless position η across the mixing layer. The dimensionless Hα emission (given by equation A7 in the text) was scaled up relatively to the dimensionless $H_2$1 — 0 S(1) emission (equation A8 in the text) by a factor 10. These results have been computed for a model with $M_j = 10$) $t_j = 0.3$ and $t_e = 0.1$.

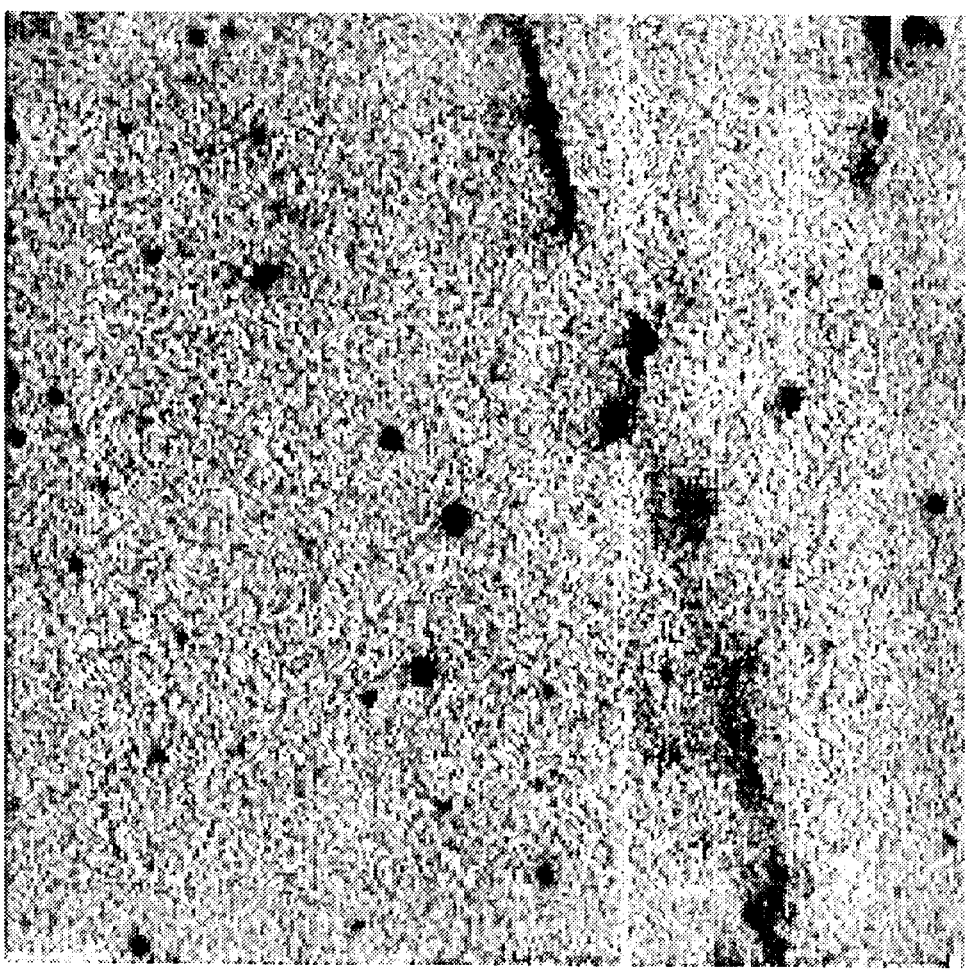

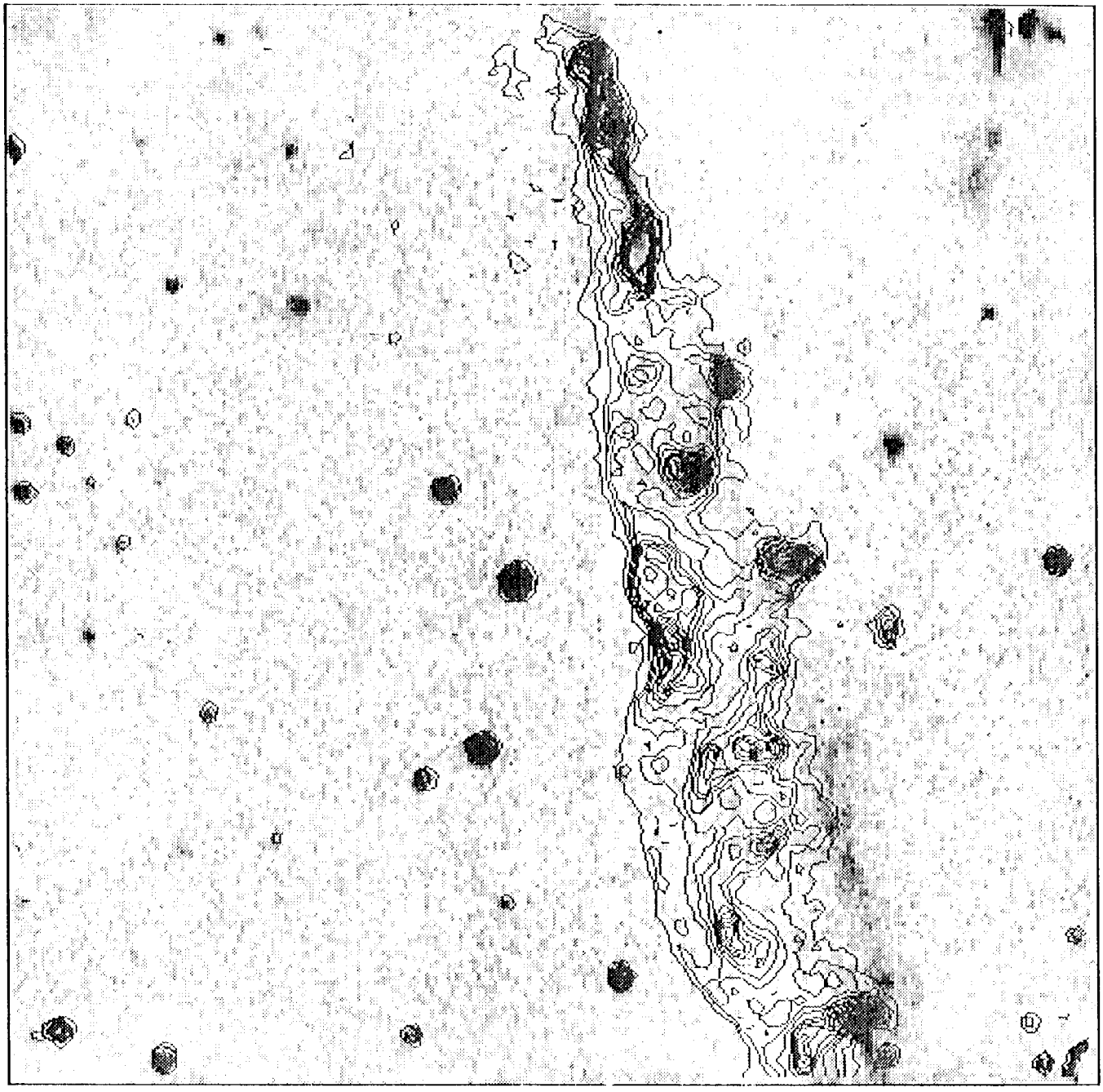

Fig 4b

Kenyon & Hartmann 1995

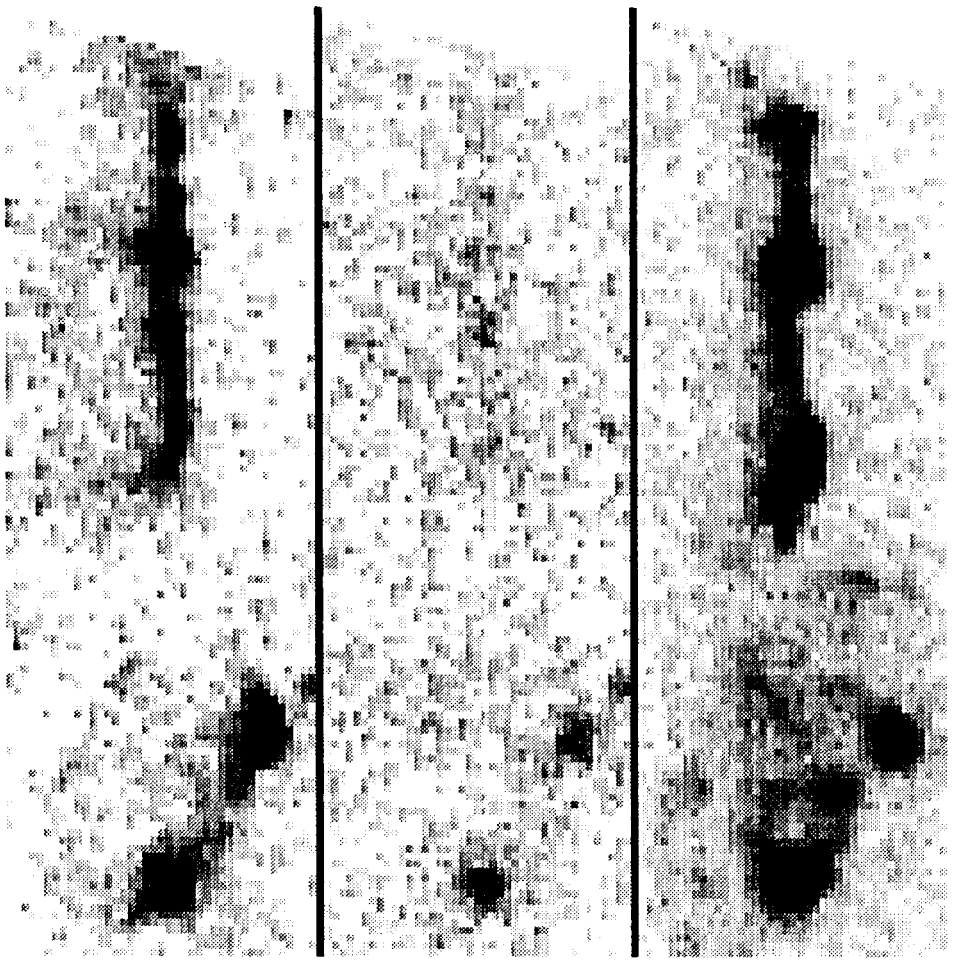

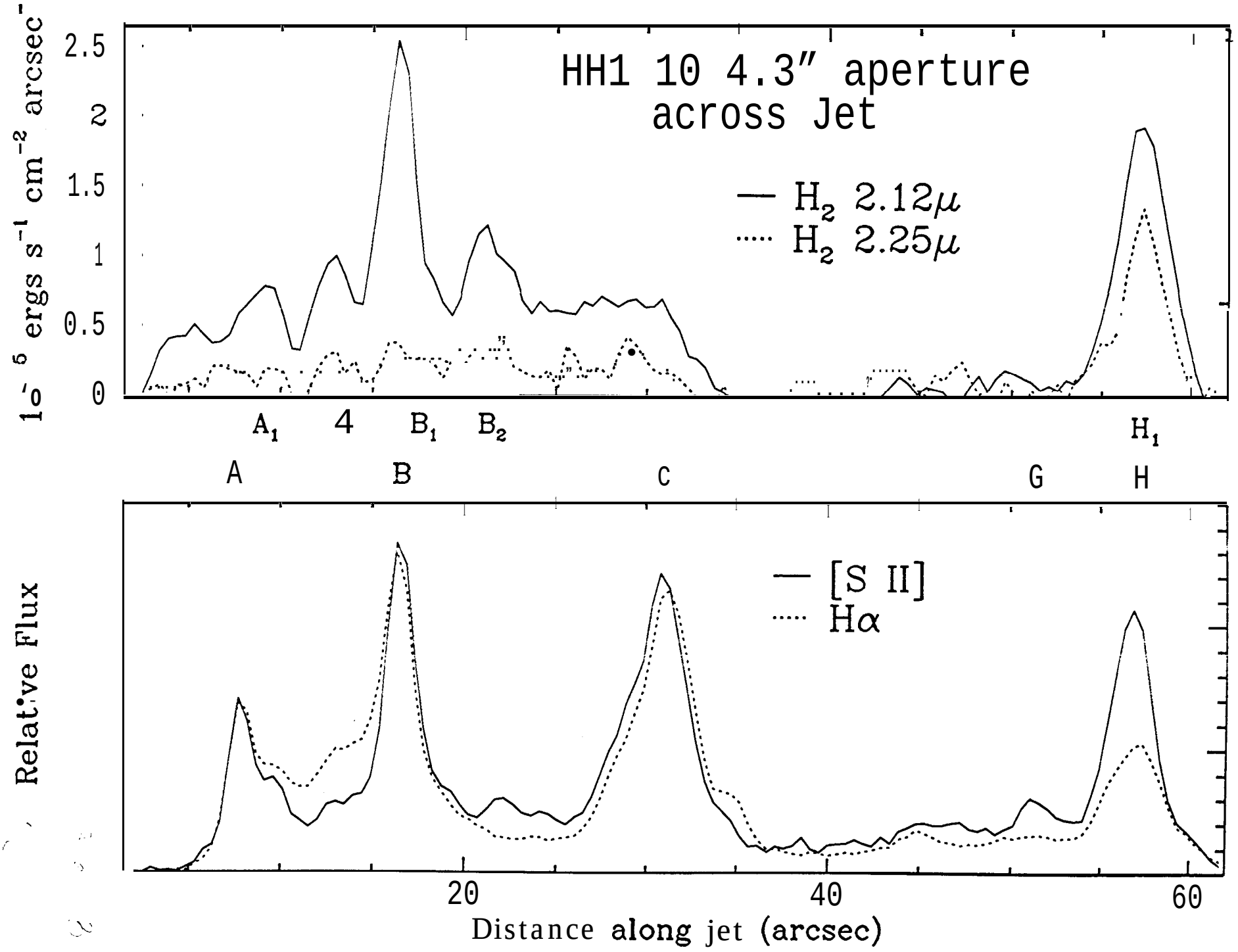
HH1 10 4.3″ aperture
across Jet
— H_2 2.12μ
····· H_2 2.25μ
10^{-5} ergs s^{-1} cm^{-2} $arcsec^{-2}$
2.5
2
1.5
1
0.5
0
A_1
4
B_1
B_2
H_1
A
B
C
G
H
— [S II]
····· Hα
Relative Flux
20
40
60
Distance along jet (arcsec)

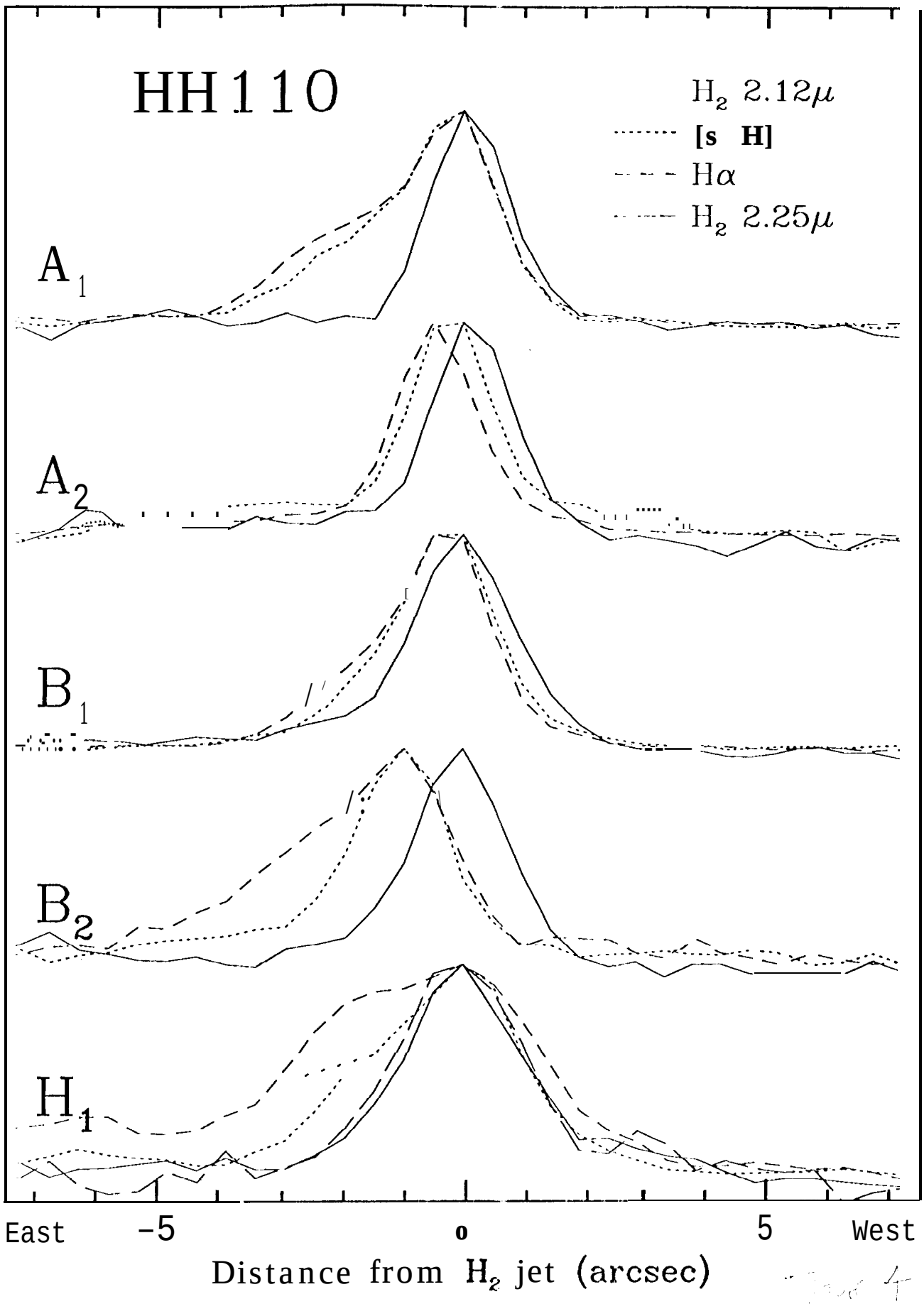
HH110
H_2 2.12μ
[s H]
Hα
H_2 2.25μ
A_1
A_2
B_1
B_2
H_1
East
-5
0
5
West
Distance from H_2 jet (arcsec)

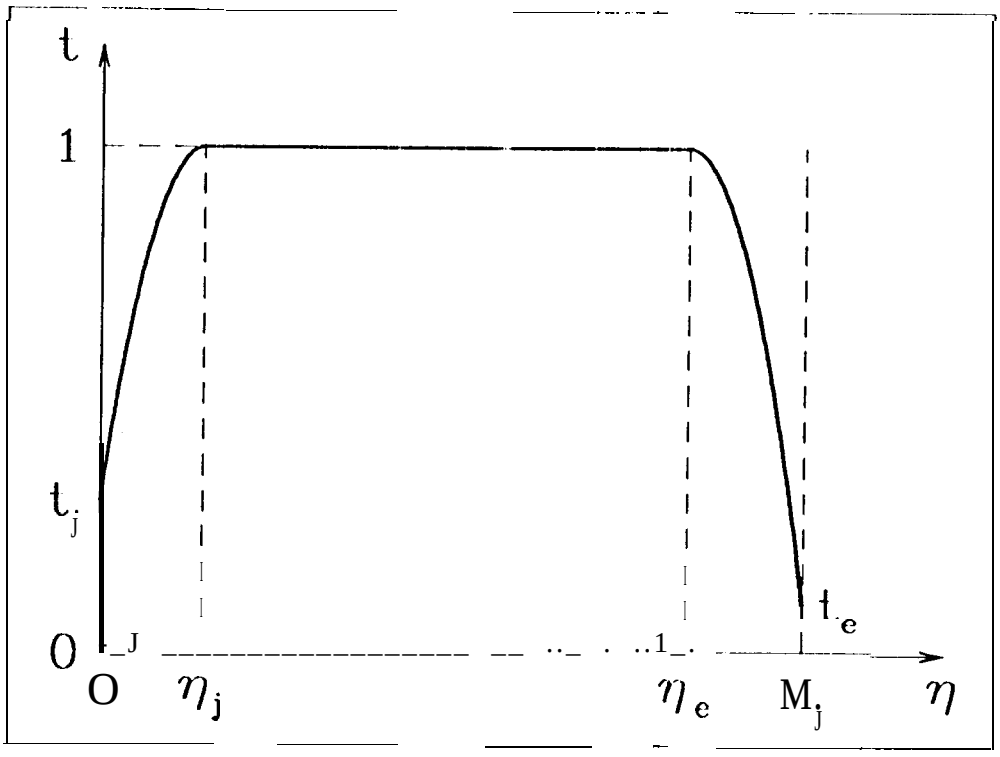

Noriega-Crespo et al. (1995)
Figure 5

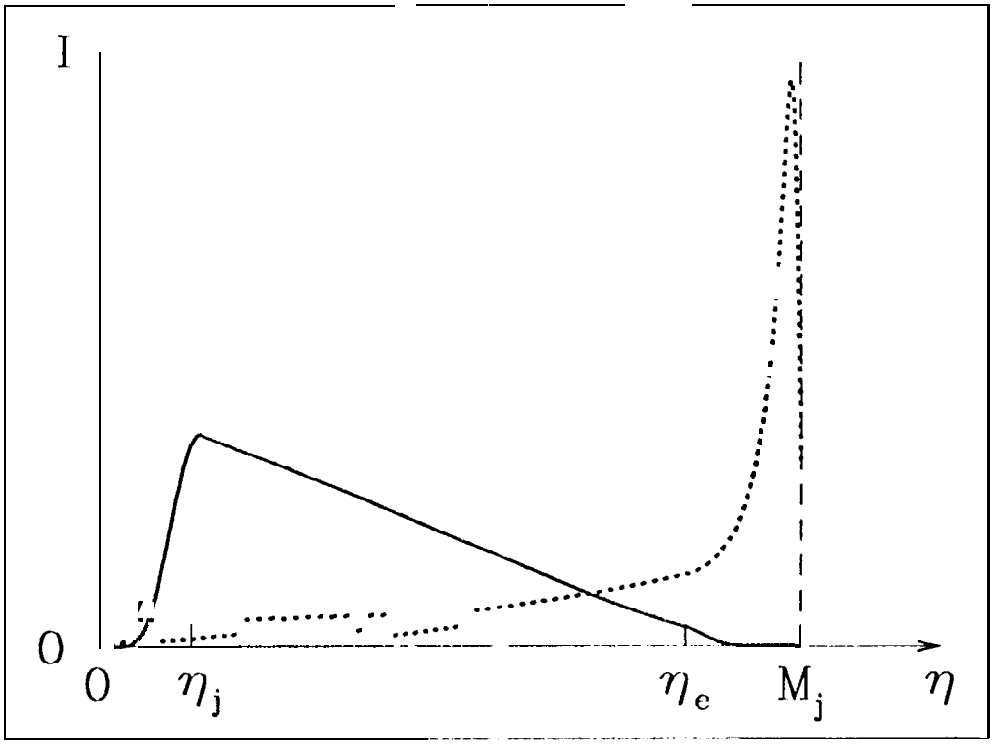

Noriega-Gropo et al. (1995)
Figure 6